Polyhedron 102 (2015) 583–592

Contents lists available at ScienceDirect

Polyhedron

journal homepage: www.elsevier.com/locate/poly

Design and synthesis of the first ferrocenylsiloxane urea: Structure and properties

Mihaela Dascalu *, Mihaela Balan, Sergiu Shova, Carmen Racles, Maria Cazacu

"Petru Poni" Institute of Macromolecular Chemistry, Aleea Gr. Ghica Voda 41 A, Iasi 700487, Romania

ARTICLE INFO

Article history:
Received 2 September 2015
Accepted 6 November 2015
Available online 14 November 2015

Keywords:
Urea
Siloxane
Ferrocene
Hydrogen-bonding
Self-assembly

ABSTRACT

The first cyclic ferrocenylsiloxane-urea, {1,1′-ferrocene-diurea-[1,3-bis(propylene)tetramethyldisiloxane]} (FSU), has been formed by reacting 1,1′-ferrocenediisocyanate with 1,3-bis(aminopropyl)-tetramethyldisiloxane in a chloroform–toluene mixture. The ferrocenylsiloxane urea was structurally characterized by FTIR and ^{1}H NMR spectroscopy, elemental analysis, mass spectrometry (ESI-MS), and single crystal X-ray diffraction. The electrochemical behavior was studied by cyclic voltammetry. FSU exhibited one reversible redox wave with a redox coupling $E_{1/2}$ = 0.107 V (FSU-$CHCl_3$), and 0.158 V (FSU-DMSO). The ^{1}H NMR analysis revealed that the ferrocenylsiloxane urea presents association capacity in chloroform, behavior sustained by transmission electron microscopy. The temperature dependence of the hydrogen bonds in the solid state complex was investigated by IR-spectroscopy.

1. Introduction

Functional unit combinations existing in material structures are responsible for their physical and chemical properties. Organometallics combine the properties of transition metal elements into organic frameworks providing access to a range of properties and geometries that are inaccessible to other organic compounds [1–5].

The synthesis, structure, electrochemistry and coordination behavior of ferrocenophanes have attracted considerable attention [6–8]. Ferrocenes are often studied because of their facile chemical modification [9], their reversible electrochemistry [10] and their strong electron donating properties [11]. The ferrocene-based receptors for anion/cation recognition are of considerable interest [12], since ferrocene exhibits a good electrochemical response due to its strong π-donating ability and good reversibility in a one-electron oxidation at a desirable range. The redox-active ferrocene moiety in the selective electrochemical sensing of anions in organic and aqueous media has been intensively studied [13–17]. Hydrogen-bond donor–receptor molecules that incorporate ferrocene have enjoyed considerable popularity as electrochemical anion sensors [18]. Also, due to the well-defined electrochemical and spectroscopic behavior, chemical stability and low toxicity of ferrocene, the compounds based on this unit have found applications in areas such as asymmetric catalysis, as mediators between redox enzymes and electrodes, as liquid crystalline materials, and in materials with high second harmonic generation efficiencies for non-linear optics [19–24].

On the other hand, urea derivatives have been intensively investigated in the area of molecular recognition due to their strong hydrogen-bonding activity. They can be used to recognize carboxylic acids, sulfonic acids, nitrates, and others through multiple-hydrogen bonding [25]. The urea group has been exploited in the construction of anion receptors [26] and is an attractive building block for anion receptors because it contains two relatively strong hydrogen-bonding sites. A variety of urea-based hosts containing one or more urea subunits have been designed and tested for anion recognition and sensing [27]. Urea-ferrocene redox-active anionophores were reported [28], for example different types of anionophores that combine the redox activity of the ferrocene moiety with the strong hydrogen-bonding ability of the urea group [29]. 1,1′-Bis(isocyanato)ferrocene was used as common building block for the preparation of these receptors. Synthesis and anion coordination properties of a new simple ferrocene-based urea receptor bearing in its structure one or two signaling units linked through two urea groups either linearly or joined through a ferrocenophane framework were reported [29].

In siloxane-urea copolymers, the presence in the structure of extremely non-polar dimethylsiloxane soft segments and very polar urea hard segments allows intermolecular hydrogen bonding with each other in the form of extended chains, with N–H "donor" groups interacting with C=O "acceptor" groups. Hydrogen bonding in urea has been the subject of numerous investigations using infrared spectroscopy [30–33]. There are various studies

* Corresponding author.
E-mail address: amihaela@icmpp.ro (M. Dascalu).

http://dx.doi.org/10.1016/j.poly.2015.11.013
0277-5387/

regarding silicon-containing organometallic compounds including the synthesis and electrochemical behavior of new classes of macromolecules containing ferrocenyl moieties together with siloxane derivates [34,35].

We report herein the product of the reaction between 1, 1′-diisocyanate-ferrocene and 1,3-bis(3-aminopropyl)tetramethyldisiloxane that proved to be a cyclic one as structural analyses revealed. The assembling through hydrogen bonds and their dynamics with temperature, concentration and solvent polarity was investigated by FTIR, ^{1}H NMR and UV–Vis. The thermal and redox behaviors were also studied.

2. Experimental

2.1. Materials

1,1′-Diisocyanateferrocene $Fc(NCO)_2$ prepared according to the procedure described in Ref. [36], was kindly offered by Prof. Matthias Tamm. 1,3-Bis(3-aminopropyl)tetramethyldisiloxane was purchased from Alfa Aesar. Toluene, chloroform, acetone and diethyl ether were reagents grade, purchased from Sigma–Aldrich and used as received.

2.2. Equipment

FT-IR spectra were recorded with Bruker Vertex 70 FT-IR spectrometer, in transmission mode with a resolution of 2 cm^{-1} and 32 scans in the 500–4000 cm^{-1} range. The ground samples were incorporated in dry KBr and processed as pellets.

The ^{1}H NMR spectra were recorded on a BRUKER Avance DRX 400 spectrometer equipped with a 5 mm QNP direct detection probe and z-gradients, using $CDCl_3$ and DMSO-d_6 as solvents. The chemical shifts are reported as δ values (ppm).

UV–Vis absorption spectra were recorded with Analytik Jena SPECORD 200 spectrophotometer using a quartz cuvette with a 1 cm path length.

Elemental analyses (C, H, N) were performed by combustion and gas chromatographic analysis with an Elementar Vario MICRO elemental analyser.

Mass spectrometry data were obtained using an Agilent 6520 Series Accurate-Mass Quadrupole Time-of-Flight (Q-TOF) LC/MS. The solutions were introduced into the electrospray ion source (ESI) via a syringe pump at a flow-rate of 0.01 mL/min. After optimization of the Q/TOF MS parameters, they were set as follows: electrospray ionization (positive ion mode), drying gas (N_2) flow rate 10.0 L/min; drying gas temperature 325 °C; nebulizer pressure 35 psig, capillary voltage 4000 V; fragmentation voltage 200 V; the full-scan mass spectra of the investigated compounds were acquired in the m/z range of 100–3000. The mass scale was calibrated using the standard calibration procedure and compounds provided by the manufacturer. The data was collected and processed using a MassHunter Workstation software.

Crystallographic measurements were carried out with an Oxford-Diffraction SuperNova diffractometer using Cu Kα radiation. The crystals were placed 40 mm from the CCD detector. The unit cell determination and data integration were carried out using the CrysAlis package of Oxford Diffraction [37]. The structure was solved by direct methods using Olex2 [38] software with the SHELXS [39] structure solution program and refined by full-matrix least-squares on F_0^2 with SHELXL-97 [39]. Atomic displacements for non-hydrogen, non-disordered atoms were refined using an anisotropic model. Two of four 3-aminopropyl fragment presented too large thermal ellipsoids, so that disordered models, in combination with the available tools (PART, DFIX, and SADI) of SHELXL-97 were applied in order to better fit the electron density. The hydrogen atoms have been placed by Fourier Difference accounting for the hybridization of the supporting atoms and the possible presence of hydrogen bonds in the case of donor atoms. The molecular plots were obtained using the OLEX2 program [38]. The main crystallographic data together with refinement details are summarized in Table S1, while the selected bond lengths and angles in Tables 2 and S2.

The thermogravimetric (TG) analysis was performed on STA 449F1 Jupiter NETZSCH equipment. The measurements were made in the 20–750 °C temperature range under a nitrogen flow (50 mL/min) using a heating rate of 10 °C/min. An Alumina crucible was used as sample holder.

Differential scanning calorimetry (DSC) measurements were conducted on a DSC 200 F3 Maia (Netzsch, Germany). The sample was heated in pressed and punched aluminum crucibles at a heating rate of 10 °C/min. Nitrogen was used as inert atmosphere at a flow rate of 100 mL/min. A heating and cooling rate of 10 °C/min was applied.

TEM investigations were made with Hitachi High-Tech HT7700 Transmission Electron Microscope, operated in high contrast mode at 100 kV accelerating voltage. Samples were cast from diluted solution (1 g/L) on 300 mesh carbon coated copper grids and vacuum dried. The cyclic voltammetry (CV) measurements were performed on a Bioanalytical System, Potentiostat–Galvanostat (BAS 100B/W).

Electrochemical experiments were carried out in a three-electrode cell consisting of a carbon glass working electrode (3 mm diameter), a platinum wire as auxiliary electrode, and a reference electrode consisting of a silver wire coated with silver chloride. Cyclic voltammograms of the investigated compounds were recorded in chloroform and DMSO solution containing tetrabutylammonium perchlorate ($TBAClO_4$) as electrolyte. All the measurements were performed at room temperature, under nitrogen atmosphere.

2.3. Synthesis of ferrocenylsiloxane urea, FSU

A 25 mL toluene solution of 1,1′-diisocyanateferrocene (Fc$(NCO)_2$) (1 g, 3.7 mmol) and a 25 mL chloroform solution of 1,3-bis(3-aminopropyl)tetramethyldisiloxane (0.93 g, 3.7 mmol) were stirred together for 24 h at room temperature. The solvent was removed under vacuum to yield a solid yellow product. The crude compound was purified by washing 3× with Et_2O. The product was filtered, and dried under vacuum to give a yellow solid (1.2 g, 65%). Suitable crystals for X-ray diffraction were obtained after crystallization in acetone. ^{1}H NMR (DMSO-d_6, 400 MHz) δ (ppm): 0.07 (s, 12H, –Si(CH_3)$_2$–O–Si(CH_3)$_2$–), 0.51 (t, J = 8.4 Hz, 4H, –CH_2–CH_2–CH_2–Si–), 1.49 (m, 4H, –CH_2–CH_2–CH_2–Si–), 3.06 (q, J = 6.2 Hz, 4H, –CH_2–CH_2–CH_2–Si–), 3.86, 4.27 (2s, 8H, Fc), 5.93 (t, J = 4.4 Hz, 2H, Fc–NH–CO–NH), 7.33 (s, 2H, Fc–NH–CO–NH). *Anal.* Calc. for dimer, according to XRD data C44H76Fe2N8O8Si4 (M_r 1069.19 g/mol): C, 49.43; H, 7.16; N, 10.48. Found: C, 49.65; H, 7.27; N, 10.38%.

3. Results and discussion

Starting with a siloxane diamine and a ferrocenediisocyanate, both di-functional monomers, one would expect a linear polymer to be formed. However, the result was different and majority cycle compound formed as single crystals, which were further characterized. In our opinion, there are three factors that could contribute to the progress of the reaction in this direction: (i) the high flexibility of the siloxane bond and angle; (ii) the amphiphilic nature of the siloxane diamine that in the non-polar reaction medium (toluene–chloroform mixture) will adopt a buckled conformation;

(iii) high dilution and stepwise adding of the second reactant in the reaction mixture. The siloxane amine was used in order to insert flexible segments with low intermolecular forces, which could give good thermal, oxidative and UV stability, high environmental and bio-compatibility [40,41], good solubility and facile processability. The structure of the formed cyclic ferrocenylsiloxane urea (FSU) (Scheme 1) was demonstrated by XRD and mass spectrometry (MS). As will be detailed below, according to XRD data the Si–O–Si angle is equal to 163.3(4) and 172.4(5) Å for A and B conformers, respectively.

3.1. X-ray crystallography

The formation of a small molecular compound was best documented with single crystal XRD. The structure analysis revealed a cyclic urea derivative, as described in Scheme 1. The X-ray single crystal study demonstrated that compound FSU has a molecular structure comprised of ferrocenylsiloxane urea and solvate water molecule in 1:1 ratio. The asymmetric unit contains two independent neutral entities (denoted as **A** and **B**) that have similar geometric parameters but differ in the conformation of the 3-aminopropyl fragment, as depicted in Fig. 1. Table 1 contain the main bonds lengths and angle and Table S2 summarizes the bonds lengths and angles.

The packing of two conformers generates a one-dimensional supramolecular column in the [100] crystallographic direction as shown in Fig. 2.

The formation of the column (Fig. 3) is directed by the intermolecular interaction, where all the N–H and O–H protons participate in the hydrogen bonding to urea oxygen atoms and solvate water molecules. The hydrogen bond parameters are displayed in Table S3.

3.2. Mass spectrometry

By positive ion ESI-mass spectrometry analysis two main peaks were detected (Fig. 1S). The peak at m/z 538.90 was attributed to the $[M-H+Na]^+$ ion, confirming the formation of a FSU without the solvate water molecule. The second peak, at m/z 1054.91 was assigned to the adduct $[2M-H+Na]^+$. The isotopic pattern of this peak corresponds with the theoretical isotopic distribution expected for this ion. ESI-MS analysis was conducted on a bulk sample. As no other species was detected at higher m/z, we concluded that the cyclic compound is the sole reaction product and linear oligomers didn't form in our reaction conditions.

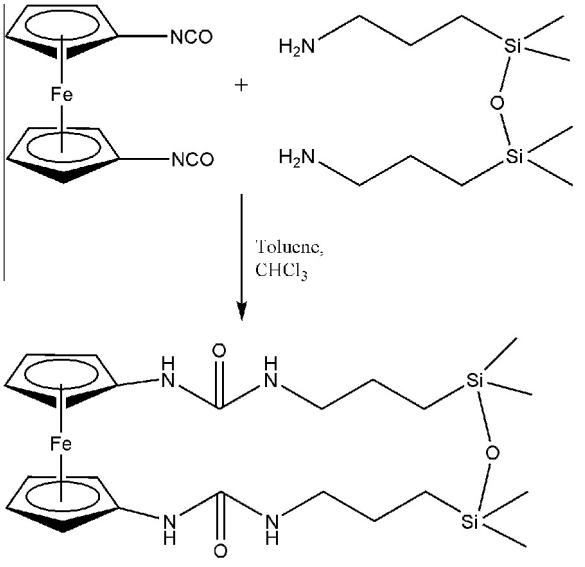

Scheme 1. Reaction scheme for the obtaining of FSU.

3.3. FTIR spectroscopy

The FTIR spectrum of the ferrocenylsiloxane urea in the 500–4000 cm^{-1} range is mainly characterized by bands at 3000–3500 cm^{-1} (NH stretching vibrations), 2800–3000 cm^{-1} (CH stretching vibrations), 1600–1800 cm^{-1} (C=O stretching vibrations), 1530 cm^{-1} (NH in plane bending) beside the bands characteristic to the siloxane segment: 2930 cm^{-1} (CH_2 antisymmetric stretch), 2860 cm^{-1} (symmetric CH_2 stretch), 1252 cm^{-1} (Si–CH_3), 1022–1078 cm^{-1} (Si–O–Si) and 798 cm^{-1} (Si–C) [32]. The absence of a peak at 2295 cm^{-1} indicates the total conversion of isocyanate groups into urea groups. The ferrocene sp^2 C–H stretching is present at around 3088 cm^{-1} while the other bands from ferrocene at 1020–1098 cm^{-1} are overlapped with the Si–O–Si band.

Besides confirming the transformation of the functional groups according to the reaction scheme, the thorough analysis of the FT-IR spectrum revealed the presence of different H-bond structures. In the compounds containing urea functional groups with N–H "donor" groups hydrogen bonded to C=O "acceptor" groups, a self-association takes place. The urea functional group has two donor (N–H) groups and one acceptor (C=O) group, the hydrogen-bonded chains consisting of 2:1 forked hydrogen bonds [30]. Some of the localized vibrations such as the N–H stretching vibrations or C=O stretching vibrations are strongly perturbed by the formation of hydrogen bonds. Both the frequency shifts and intensities changes are measures of the specificity or magnitude of the formed hydrogen bonds [32]. Fourier transform infrared (FTIR) and variable-temperature FTIR spectroscopy are the main methods for characterizing hydrogen bonding and its thermal motion [31,42–45]. The extent of hydrogen bonding in urea compounds can qualitatively be studied by determining the frequency shifts in hydrogen bonded –N–H and –C=O peaks –N–H···O=C relative to the free –N–H and –C=O peaks. The shifts in these peaks to lower frequencies result from the weakening of the bonds between N–H and C=O groups due to hydrogen bonding. The self-association in urea compounds is stronger than in urethane ones as a result of the formation of bifurcated (as opposed to linear) hydrogen bonds [46–48].

Temperature dependent IR-spectra of ferrocenylsiloxane urea in the 1600–1800 cm^{-1} range are shown in Fig. 4. The figure illustrates the changes of the absorption bands (maxima) of the carbonyl groups. The weak shoulder around 1650 cm^{-1} and the band at 1698 cm^{-1} are attributed to the disordered hydrogen-bonded urea carbonyl. The band at 1744 cm^{-1} (at 100 °C) is temperature dependent and attributed to the free urea carbonyl. This band returns to its initial intensity after cooling. The band from 1634 cm^{-1} corresponds to the hydrogen-bonded ordered urea carbonyl [32,33]. A small increase of the relative intensity with the increasing temperature can be seen.

The FTIR spectra of FSU in the N–H stretching region, recorded as a function of temperature in the 3000–3500 cm^{-1} range, are shown in Fig. 5. There is a similar trend for N–H stretching with increasing temperature: the band shifts to higher wavenumber and the intensity of the band decreases. Due to the strong dependence of absorption coefficient on temperature, the decrease of intensity of the hydrogen bonded N–H stretching band does not reveal a direct change of the strength of hydrogen bonding. However, the distribution of hydrogen bonded groups at different distances and geometries has been described as follows: the broader the band is, the more disordered the hydrogen bonds are in the sample [31,45,49]. In our case, there is a narrowing tendency for this band with increasing temperature, which would mean increasing order. This is in agreement with the increase of the "C=O ordered" absorbance, as observed in Fig. 4.

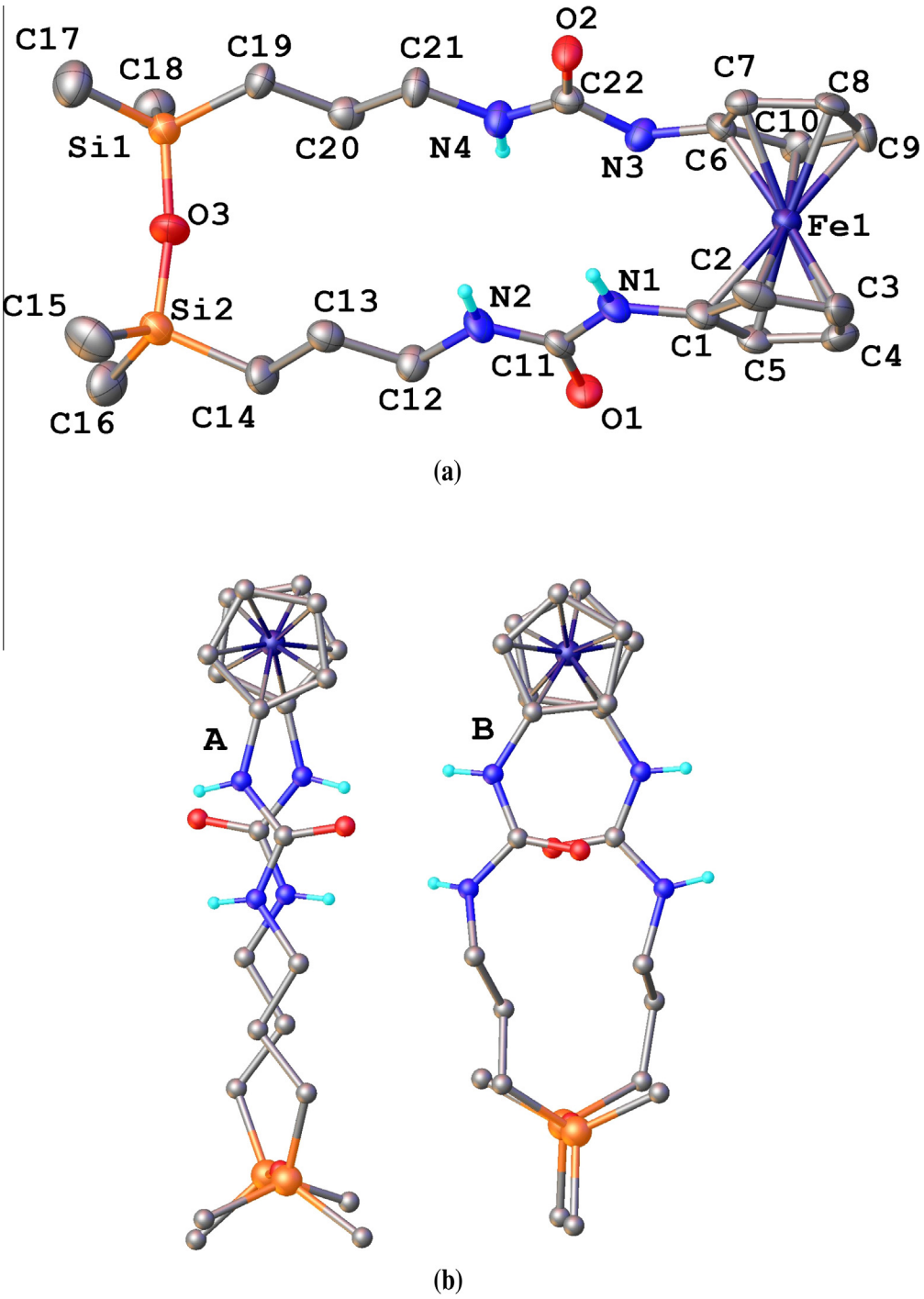

Fig. 1. (a) Atom labeling scheme used for two asymmetric molecules (shown on the base of component **A**). Thermal ellipsoids are drawn at 30% probability level. (b) View of two conformers **A** and **B**. Non-relevant hydrogen atoms are omitted for clarity.

A summary of the main bands assignment for the urea carbonyl and N–H stretching modes is presented in Scheme 2.

The band at around 3725 cm^{-1} is assigned to free OH groups (from crystallization water). In the FTIR spectra of the FSU recorded from 25 to 100 °C, it can be observed the intensification of this band as the temperature increases (Fig. 6).

3.4. ^1H NMR spectroscopy

The ^1H NMR spectrum recorded in DMSO-d_6 indicated the formation of the ferrocenylsiloxane-urea compound. The ratio of the peaks intensities of the protons from Fc and siloxane units indicate that the two components are in a molar ratio of 1:1 in the final product. The protons of the central methylene group of the propyl chains are observed as a multiplet at 1.49 ppm. A triplet, corresponding to the methylene protons adjacent to the siloxane groups, appears at 0.51 ppm, the methylene protons adjacent to the urea groups are observed as a multiplet at 3.06 ppm, while the dimethylsiloxane protons appear at 0.07 ppm. Two signals are observed for the ferrocenyl protons. All four of the *m*-protons appear as a singlet at 4.27 ppm, while the four *o*-protons are observed as a singlet at 3.86 ppm.

Table 1
Selected bond lengths (Å) and angles (°).

	Molecule A	Molecule B
Distances		
Si1–O3	1.611(5)	1.615(6)
Si2–O3	1.614(5)	1.603(6)
C1–N1	1.406(8)	1.404(8)
C6–N3	1.404(8)	1.414(8)
N1–C11	1.364(7)	1.346(9)
N4–C22	1.323(8)	1.352(9)
N3–C22	1.371(8)	1.320(9)
N4–C21	1.462(7)	1.508(5)
N2–C11	1.321(8)	1.360(9)
N2–C12	1.508(5)	1.508(5)
O2–C22	1.241(7)	1.233(9)
O1–C11	1.244(7)	1.214(9)
Angles		
O2–C22–N3	120.6(6)	123.4(8)
O2–C22–N4	123.7(7)	123.6(8)
O3–Si1–C19	107.9(3)	109.2(4)
O3–Si2–C14	107.1(3)	109.4(4)
N1–C11–O1	121.6(6)	122.4(8)
N1–C11–N2	114.9(6)	113.6(7)
N2–C11–O1	123.6(6)	124.0(8)
N3–C22–N4	115.7(6)	113.0(7)
C1–N1–C11	125.9(6)	126.6(6)
C6–N3–C22	127.3(6)	125.6(6)
C11–N2–C12	119.6(6)	121.3(8)
C21–N4–C22	121.3(6)	119.8(8)
Si1–O3–Si2	169.3(4)	172.4(5)

In general, one can expect the existence of an equilibrium between intermolecular H-bonded and non-H-bonded states in solution but the equilibrium is too fast for the NMR timescale and we observe average δ values between free and hydrogen-bonded species. Non-polar solvents, such as $CDCl_3$, favor intermolecular H-bonded structures, while polar solvents such as DMSO disrupt H-bonding by competing with the H-bonding sites. To

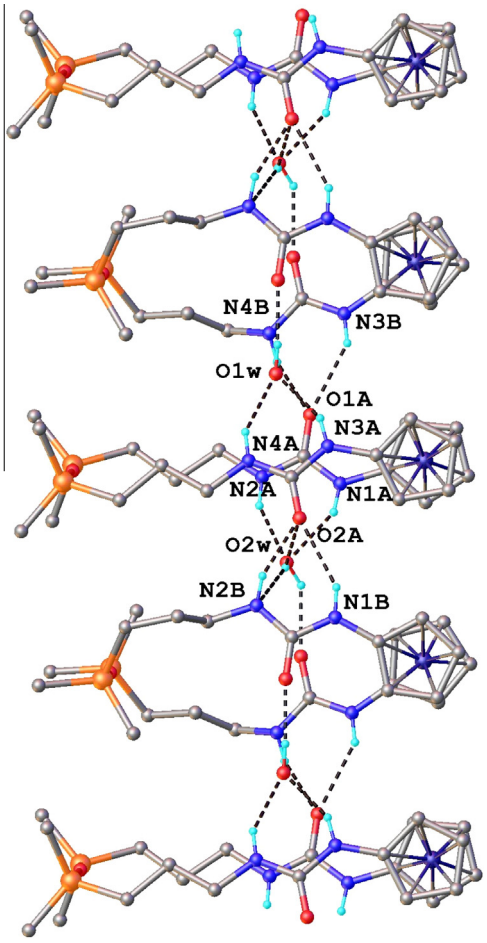

Fig. 3. Extensive hydrogen bonding in crystal structure FSU.

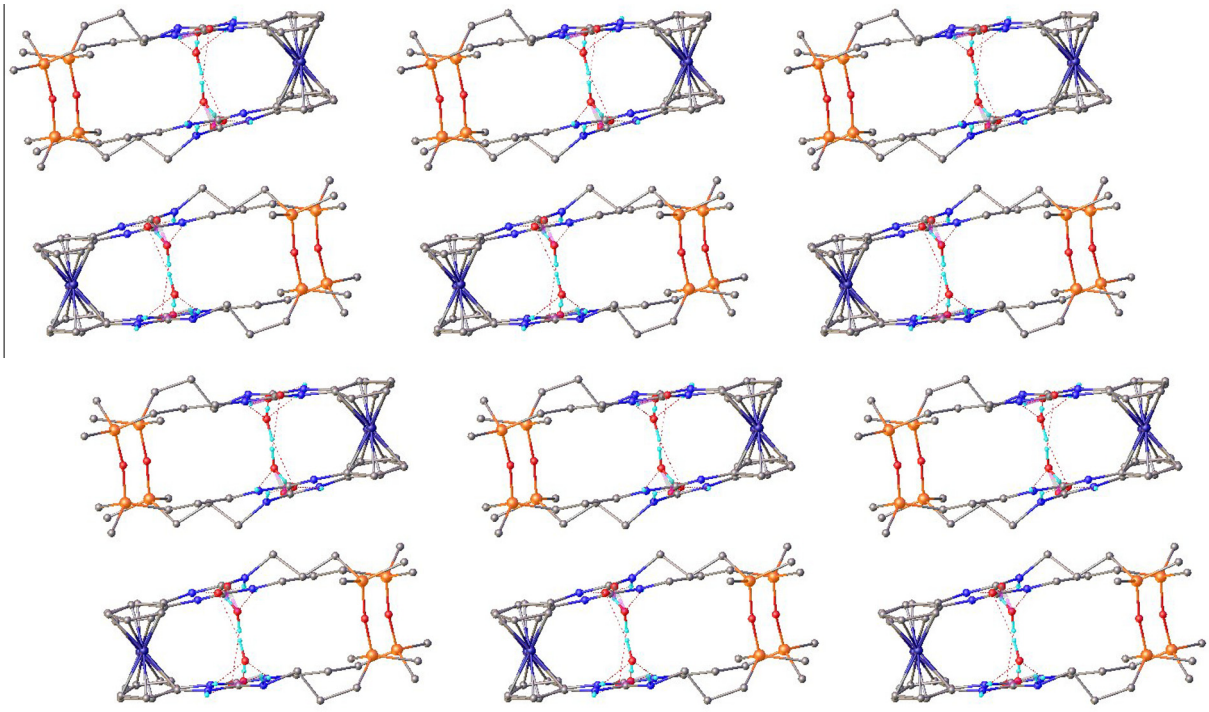

Fig. 2. View of the crystal structure along *a* crystallographic direction.

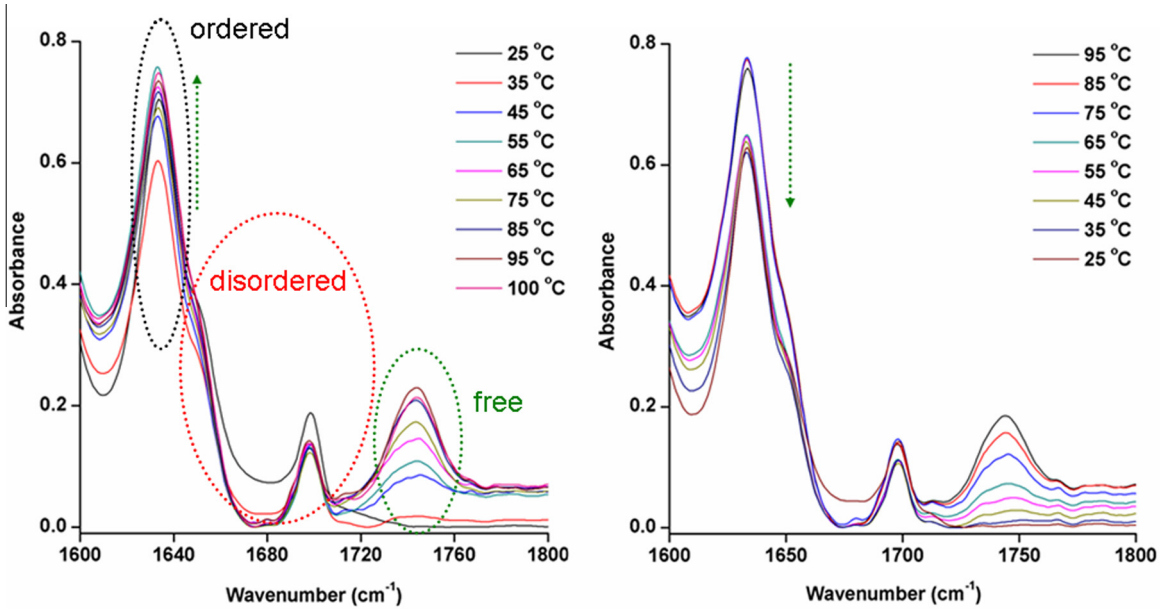

Fig. 4. FTIR spectra of the C=O urea region of FSU recorded from 25 to 100 °C in the range 1600–1800 cm^{-1} (left-heating, right-cooling).

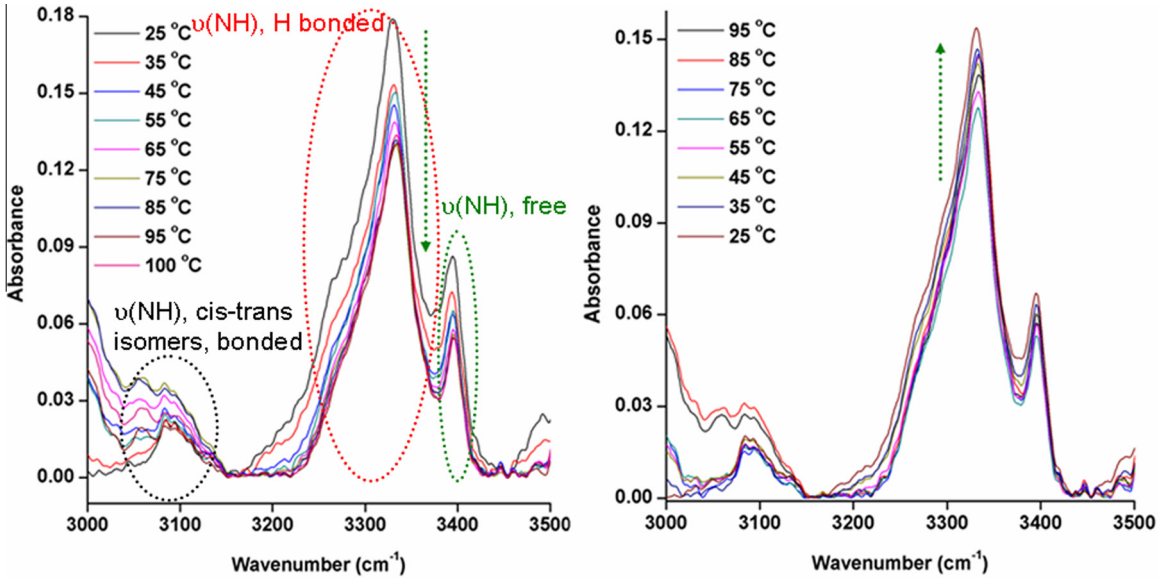

Fig. 5. FTIR spectra of the N–H stretching region of FSU recorded from 25 to 100 °C in the 3000–3500 cm^{-1} range (left-heating, right-cooling).

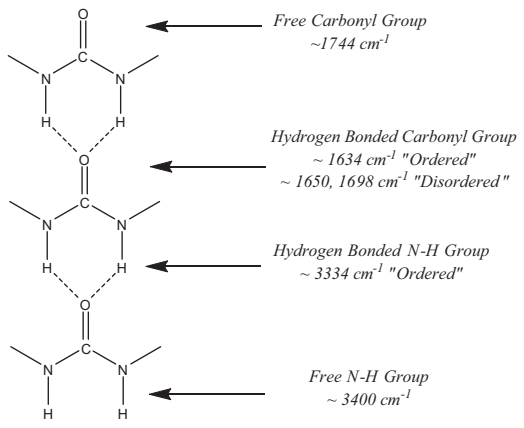

Scheme 2. Band assignments for the urea carbonyl and N–H stretching modes.

observe the H-bonding of FSU in solution, NMR measurements were carried out in pure $CDCl_3$, pure DMSO-d_6, and mixture thereof in various proportions.

Fig. 7 shows the concentration dependence of the chemical shift of the –N*H* protons of FSU in $CDCl_3$–DMSO-d_6 mixtures (Table 2). In $CDCl_3$ solution (*C*0), compound FSU exhibits one visible urea resonance at δ 5.14 ppm for the FcNHCON*H*– and one at ~7.2 ppm FcN*H*CONH– overlapped by $CDCl_3$ peak. An ordered conformation is adopted by these compounds in non-polar solution, via the formation of intermolecular hydrogen bonds. Starting from *C*1, the peaks assigned to the protons from urea groups are easily detectable. There is a shift of the peaks assigned to FcNHCON*H*– from 5.14 (*C*0) to 5.48 (*C*1) and 5.88 ppm (*C*8) with the progressive addition of DMSO-d_6. In *C*8, (DMSO-d_6 majority solvent), the resonances at δ 5.88 (FcNHCON*H*–) and 7.30 (FcN*H*CONH–) are observed. The chemical shift differences for the two urea protons in the two solvents are $\Delta\delta = 0.74$ for the FcNHCON*H*– and $\Delta\delta = 0.1$ for the FcN*H*CONH– group. Self-association and

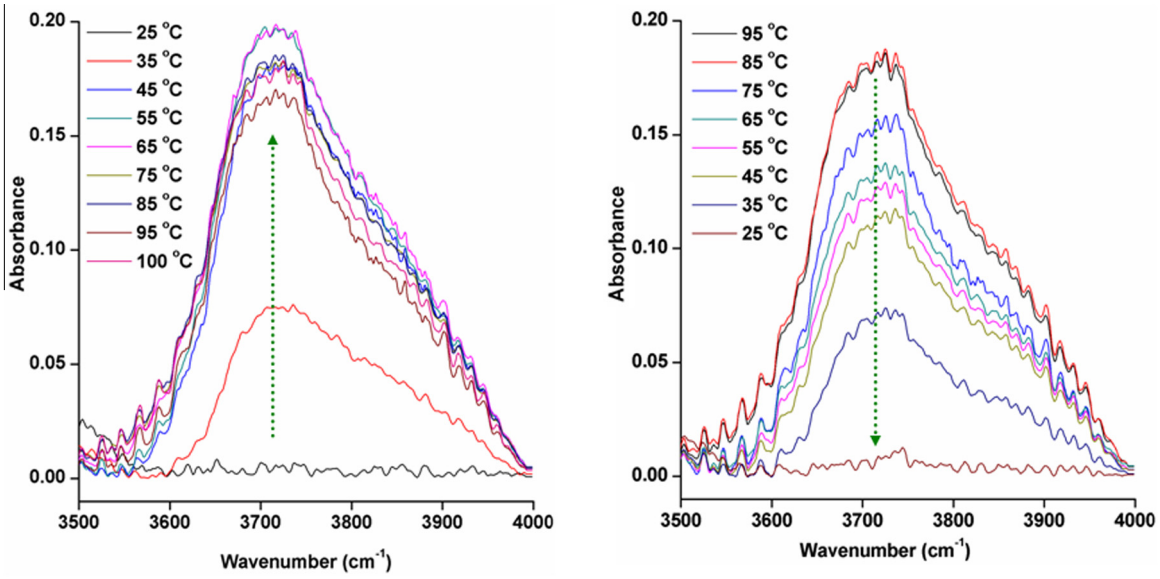

Fig. 6. FTIR spectra of the OH stretching region of FSU recorded from 25 to 100 °C in the 3500–4000 cm^{-1} range (left-heating, right-cooling).

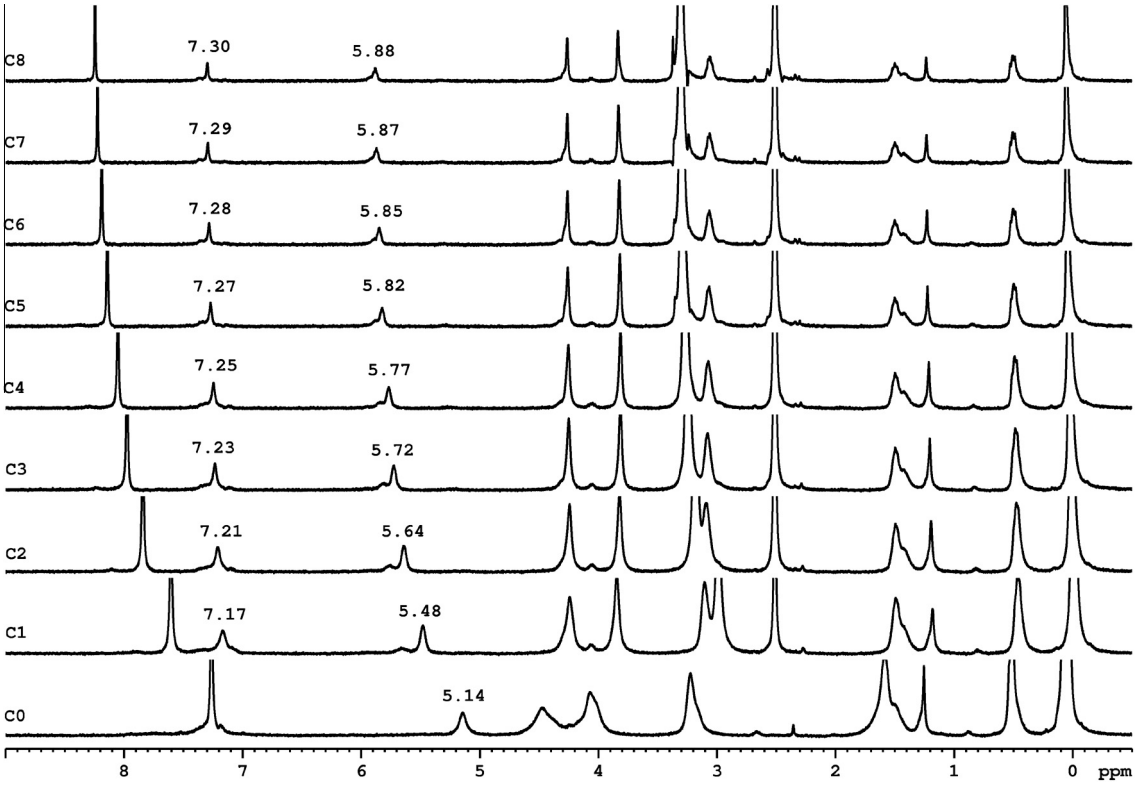

Fig. 7. ^{1}H NMR spectra of FSU in pure $CDCl_3$ (C0) and in solvent mixture in different proportion $CDCl_3$:DMSO-d_6 (C1–C8).

interaction with a good hydrogen-bond accepting solvent have a significant effect on the N–H proton chemical shifts of FSU.

3.5. UV–Vis spectroscopy

The electron absorption spectra of FSU were recorded at different concentrations in order to follow the changes occurring in the intensity of the absorption bands. The UV–Vis spectra of FSU show high energy bands at 433, 629 and 861 nm at room temperature in $CHCl_3$. The band at 433 nm is attributed to d–d electronic transition of the ferrocene unit, and it is more dependent on concentration then the other two bands. The ligand-to-metal charge transfer (LMCT) transition at 629 nm indicates the presence of ferrocenium centers. With increasing concentration of FSU, a gradual increase in the intensity of all the bands was observed as shown in Fig. 8a. The changes in the absorbance bands with the concentration of FSU in $CHCl_3$ are shown in the three curves of Fig. 8b.

3.6. Thermal analysis

Thermogravimetric studies were performed on FSU in the 25–700 °C temperature range, under nitrogen atmosphere

Table 2
The amount of reactants and solvents used for the ^{1}H NMR studies.

Code	Concentration (mM)	Amount of solvent	
		$CDCl_3$ (mL)	DMSO-d_6 (mL)
C0	4.90	0.6	0
C1	4.30	0.6	0.1
C2	3.75	0.6	0.2
C3	3.33	0.6	0.3
C4	3.00	0.6	0.4
C5	2.73	0.6	0.5
C6	2.30	0.6	0.7
C7	2.00	0.6	0.9
C8	1.77	0.6	1.1

(Fig. 2S). The initial weight loss of 19% in the 103–297 °C temperature window is attributed to the removal of water and solvents molecules. Upon increasing the temperature, a further weight loss of ~10% was observed up to 510 °C attributed to the pyrolysis of the organic part of the compound. The large amount of residue is presumably due to the formation of silicon and iron oxides [50]. Two relatively broad endothermic peaks were observed at 76 and 125 °C on DSC trace (Fig. 3S), that are assigned to the dissociation of the hydrogen bonds and to the melting transition of the low-ordered stiff segments. In the second run, these peaks are not so evident, which probably means that the urea molecules haven't had sufficient time to rearrange during the relatively fast cooling of the sample in the calorimeter.

3.7. Transmission electron microscopy

The ferrocenylsiloxane urea samples cast from $CHCl_3$ and DMSO solutions were investigated by TEM. Taking into account the structure of FSU and the information obtained from the ^{1}H NMR study, one should expect a different aspect of the films generated from $CHCl_3$ and DMSO solutions. As discussed before, $CHCl_3$ would favor H bonding of urea groups, while DMSO would impede this. Indeed a different aspect of the drop cast samples was observed by TEM, after fast removal of the solvent. In the case of $CHCl_3$, quasi-spherical aggregates are observed (Fig. 9) with vesicle-like aspect. This morphology is confirmed by the EDX analysis on a line crossing the formation, which reveals the presence of both Fe and Si in the walls of the aggregate. Due to the presence of the urea groups, hydrogen bonding is the essential phenomenon leading to the self-assembly of the polar domains. When the evaporation of the solvent was conducted under chloroform saturated atmosphere, the TEM images of FSU are different from those obtained by fast solvent removal. In this case FSU is organizing as crystallites (Fig. 10).

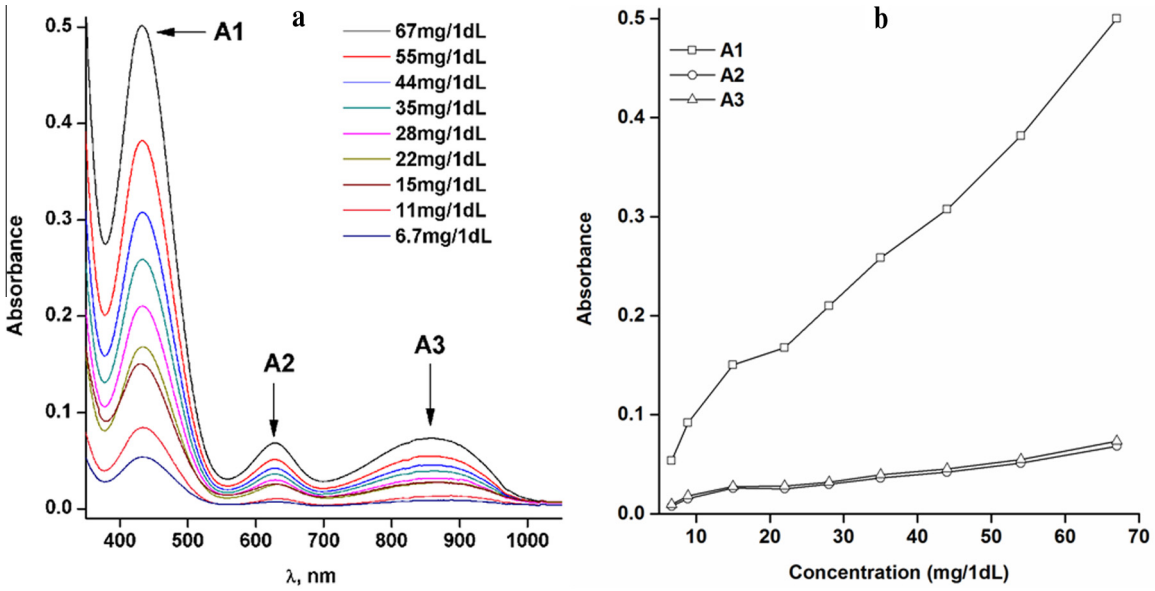

Fig. 8. Change in electronic spectra of FSU with concentration in $CHCl_3$ solution (a), dependence of the maximum absorbance on the concentration (b).

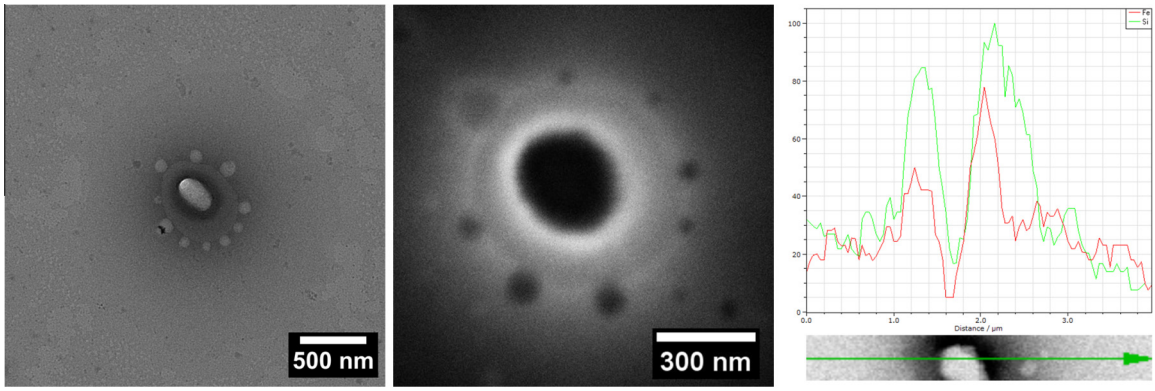

Fig. 9. TEM and STEM images of FSU cast from $CHCl_3$ (fast removal of the solvent); the right-side picture is the EDX analysis on a line.

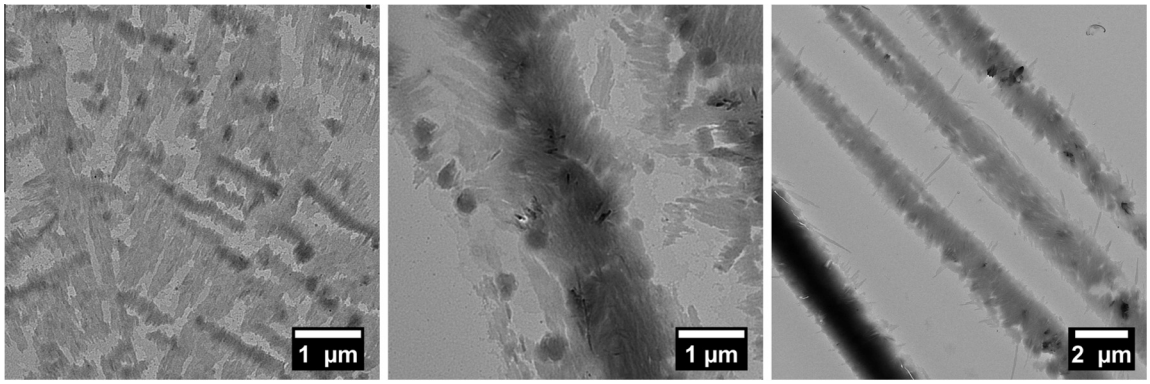

Fig. 10. TEM images of FSU thin films cast from $CHCl_3$ (evaporation of the solvent under saturate atmosphere).

In a polar solvent such as DMSO, the polar domains consisting in ferrocene-urea moieties will orient towards the solvent while the non-polar parts will obey their natural tendency to minimize the contact with such a solvent. In the TEM images of FSU drop-casted from DMSO no clear indication of self-association was observed (Fig. 4S).

3.8. Electrochemistry studies

The electrochemical properties of ferrocenylsiloxane urea were studied by cyclic voltammetry in chloroform and DMSO containing $TBAClO_4$ (0.1 M) as supporting electrolyte. The potential value applied to the working electrode was swept in a large window potential, with a 50 mV/s scan rate. The cyclic voltammograms recorded in the two solvents are shown in Fig. 11. The recorded curves indicate that the synthesized ferrocenylsiloxane urea exhibits quasi-reversible one-electron oxidation process vs. ferrocenium–ferrocene (Fe^+/Fe) couple and the electrochemical data are listed in Table 3.

The voltammograms indicate one reversible redox process with an anodic peak potential (E (V)) of 0.196 V for FSU-DMSO, and 0.194 V for FSU-$CHCl_3$. The electrons removal in the oxidation step is assumed to ferrocene units and the values of ΔE are 2 times higher (FSU-$CHCl_3$) or closer (FSU-DMSO) compared to the ferrocene (Fc) single molecule (ΔE = 0.083 V). FSU shows good reversibility of redox processes having half-wave potential at $E_{1/2}$ = 0.107 V (FSU-$CHCl_3$), and 0.158 V (FSU-DMSO) vs. Ag/AgCl, respectively. The detection of single reversible oxidation waves indicates that in these compounds the iron centers are essentially noninteracting.

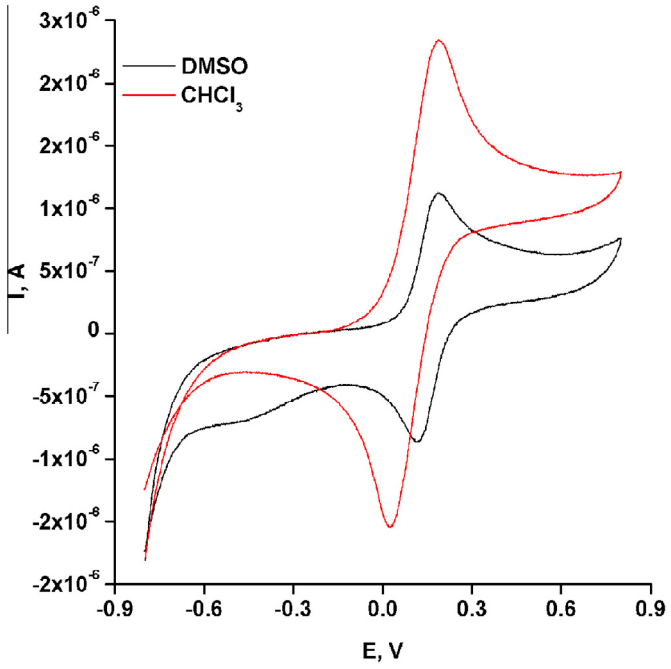

Fig. 11. Cyclic voltammograms for FSU in $CHCl_3$ and DMSO solutions; scan rate = 50 mV/s.

Table 3
Electrochemical data of ferrocene and FSU in different solvents.

E/V	Sample		
	Fc	FSU-$CHCl_3$	FSU-*DMSO*
E_{pa}	0.556	0.194	0.196
E_{pc}	0.473	0.020	0.110
ΔE	0.083	0.174	0.086
$E_{1/2}$	0.525	0.107	0.158

E_{pa} – anodic peak potential; E_{pc} – cathodic peak potential, ΔE – the peak separation ($\Delta E = E_{pa} - E_{pc}$), $E_{1/2}$ – the half-wave potential ($E_{1/2} = (E_{pa} + E_{pc})/2$).

5. Conclusions

By reacting 1,1′-ferrocenediisocyanate with 1,3-bis(aminopropyl)tetramethyldisiloxane, {1,1′-ferrocene-diurea-[1,3-bis(propylene)tetramethyldisiloxane]} FSU, was formed and X-ray single crystal diffraction and spectral (IR, ^{1}H NMR, UV–Vis and MS) data were obtained. The asymmetric unit contains two conformers packed in one-dimensional supramolecular column through intermolecular interaction between N–H and O–H protons on the one hand with urea oxygen atoms and solvate water molecules on the other hand. FTIR spectra confirmed the structure of the compounds and its assembling by hydrogen bonds that are dependent on the temperature. A reversible breaking of the hydrogen bonds occurs in the solid state as the temperature increases to 100 °C. ^{1}H NMR spectra revealed the dependence of the chemical shifts of the groups responsible on the hydrogen bond formation on concentration and solvent polarity. After the loss of crystalline water and retained solvent traces, the compound is stable up to 510 °C when the organic part is decomposed leaving a large amount of residue consisting in iron and silicon oxides. Due to the co-existence in structure of the polar (ferrocenyl-urea) and non-polar (bis(propyl)tetramethyldisiloxane) moieties, the compound proved to be able to self-assemble in $CHCl_3$ in quasi-spherical aggregates with vesicle-like aspect. This behavior was less obvious in polar medium (DMSO). The compound showed reversible redox processes and the shape of the voltammogram indicates the presence of essentially noninteracting iron centers in structure.

Acknowledgments

This work was supported by a grant of the Ministry of National Education, CNCS-UEFISCDI, project number PN-II-ID-PCE-2012-4-0261, and from European Union's Seventh Framework Programme (FP7/2007-2013) under grant agreement n°264115 – STREAM. We gratefully acknowledge Prof Matthias Tamm from Institut für Anorganische und Analytische Chemie, Technische Universität Braunschweig, Germany for providing us 1,1′-diisocyanatoferrocene. We also like to acknowledge Dr. M.F. Zaltariov for FTIR measurements, Dr. L. Vacareanu for electrochemistry measurements, Dr. L. Sacarescu for TEM measurements and Dr. M. Silion for mass-spectrometry measurements.

Appendix A. Supplementary data

CCDC 1060113 contain the supplementary crystallographic data for FSU. These data can be obtained free of charge via http://www.ccdc.cam.ac.uk/conts/retrieving.html, or from the Cambridge Crystallographic Data Centre, 12 Union Road, Cambridge CB2 1EZ, UK; fax: (+44) 1223-336-033; or e-mail: deposit@ccdc.cam.ac.uk. Supplementary data associated with this article can be found, in the online version, at http://dx.doi.org/10.1016/j.poly.2015.11.013.

References

[1] D.A. Wilson, G. Lisa, D. Scutaru, N. Hurduc, J. Iran. Chem. Soc. 8 (2011) 782.
[2] O.N. Kadkin, E.H. Kim, S.Y. Kim, M.-G. Choi, Polyhedron 28 (2009) 1301.
[3] C. Lisa, S. Curteanu, V. Bulacovschi, D. Apreutesei, Rev. Roum. Chim. 53 (2008) 283.
[4] H.W. Chae, O.N. Kadkin, M.-G. Choi, Liq. Crystallogr. 36 (2009) 53.
[5] O.N. Kadkin, H. Han, Y.G. Galyametdinov, J. Organomet. Chem. 692 (2007) 5571.
[6] P.D. Beer, Z. Chen, M.G.B. Drew, A.O.M. Johnson, D.K. Smith, P. Spencer, Inorg. Chim. Acta 246 (1996) 143.
[7] T. Moriuchi, I. Ikeda, T. Hirao, Organometallics 14 (1995) 3578.
[8] L.-Y. Zhang, Y.-F. Yuan, A.-G. Hu, J.-T. Wang, J. Sun, J. Organomet. Chem. 637–639 (2001) 204.
[9] (a) A. Hildebrandt, T. Rüffer, E. Erasmus, J.C. Swarts, H. Lang, Organometallics 29 (2010) 4900;
(b) F. Rebiere, Tetrahedron Lett. 31 (1990) 3121.
[10] (a) N.G. Connelly, W.E. Geiger, Chem. Rev. 96 (1996) 877;
(b) A. Auger, A.J. Muller, J.C. Swarts, Dalton Trans. (2007) 3623.
[11] (a) S. Otto, A. Roodt, J.J.C. Erasmus, J.C. Swarts, Polyhedron 17 (1998) 2447;
(b) A.A.O. Sarhan, O.F. Mohammed, T. Izumi, Beilstein J. Org. Chem. 5 (6) (2009) 1.
[12] (a) Q.-Y. Cao, M.H. Lee, J.F. Zhang, W.X. Ren, J.S. Kim, Tetrahedron Lett. 52 (2011) 2786;
(b) Q.-Y. Cao, J.F. Zhang, W.X. Ren, K. Choi, J.S. Kim, Tetrahedron Lett. 52 (2011) 4464;
(c) Q.-Y. Cao, T. Pradhan, S. Kim, J.S. Kim, Org. Lett. 13 (2011) 4386.
[13] P.D. Beer, P.A. Gale, G.Z. Chen, J. Chem. Soc., Dalton Trans. (1999) 1897.
[14] P.D. Beer, J.A. Cadman, Coord. Chem. Rev. 205 (2000) 131.
[15] O. Reynes, J. Moutet, J. Pecaut, G. Royal, E. Saint-Aman, New J. Chem. 26 (2002) 9.
[16] A. Labande, J. Ruiz, D. Astruc, J. Am. Chem. Soc. 124 (2002) 1782.
[17] P.D. Beer, M.G.B. Drew, D. Hesek, K.C. Nam, Organometallics 18 (1999) 3933.
[18] N.H. Evans, C.J. Serpell, K.E. Christensen, P.D. Beer, Eur. J. Inorg. Chem. (2012) 939.
[19] D. Nieto, A.M. Gonźalez-Vadillo, S. Brũna, C.J. Pastor, A.E. Kaifer, I. Cuadrado, Chem. Commun. 47 (2011) 10398.
[20] M. Fuentealba, J.-R. Hamon, D. Carrillo, C. Manzur, New J. Chem. 31 (2007) 1815.
[21] S.K. Pal, A. Krishnan, P.K. Das, A.G. Samuelson, J. Organomet. Chem. 604 (2000) 248.
[22] L. Mishra, S.-K. Dubey, Spectrochim. Acta, Part A 68 (2007) 364.
[23] A.-E. Navarro, N. Spinelli, C. Moustrou, C. Chaix, B. Mandrand, H. Brisset, Nucleic Acids Res. 32 (2004) 5310.
[24] S.R. Bayly, P.D. Beer, G.Z. Chen, in: P. Štěpnička (Ed.), Ferrocenes: ligands, materials and biomolecules, Wiley, UK, 2008, pp. 281–318;
b) S.K. Kim, D.H. Lee, J.-I. Hong, J. Yoon, Acc. Chem. Res. 42 (2009) 23;
c) J.W. Steed, Chem. Soc. Rev. 38 (2009) 506;
d) R.M. Duke, E.B. Veale, F.M. Pfeffer, P.E. Kruger, T. Gunnlaugsson, Chem. Soc. Rev. 39 (2010) 3936.
[25] Y. Takemoto, Org. Biomol. Chem. 3 (2005) 4299.
[26] M.D. Pratt, P.D. Beer, Polyhedron 22 (2003) 649.
[27] (a) C.R. Bondy, P.A. Gale, S.J. Loeb, J. Am. Chem. Soc. 126 (2004) 5030;
(b) L.Y. Lee, E.J. Cho, S. Mukamel, K.C. Nam, J. Org. Chem. 69 (2004) 943;
(c) J.Y. Kwon, Y.J. Jang, S.K. Kim, K.-H. Lee, J.S. Kim, J. Yoon, J. Org. Chem. 69 (2004) 5155;
(d) D.A. Jose, D.K. Kumar, B. Ganguly, A. Das, Tetrahedron Lett. 46 (2005) 5343;
(e) D. Esteban-Gomez, L. Fabbrizzi, M. Licchelli, J. Org. Chem. 70 (2005) 5717;
(f) M. Boiocchi, L. Del Boca, D. Esteban-Gomez, L. Fabbrizzi, M. Licchelli, E. Monzani, Chem. Eur. J. 11 (2005) 3097.
[28] (a) H. Miyaji, S.R. Collinson, I. Prokes, J.H.R. Tucker, Chem. Commun. (2003) 64;
(b) F. Otón, A. Tárraga, A. Espinosa, M.D. Velasco, D. Bautista, P. Molina, J. Org. Chem. 70 (2005) 6603.
[29] F. Otón, A. Tárraga, A. Espinosa, M.D. Velasco, Pedro Molina, J. Org. Chem. 71 (2006) 4590.
[30] J. Mattia, P. Painter, Macromolecules 40 (2007) 1546.
[31] L. Lanjie, Y. Guisheng, Polym. Int. 58 (2009) 503.
[32] D.P. Queiroz, M.N. de Pinho, C. Dias, Macromolecules 36 (2003) 4195.
[33] E. Yilgör, E. Burgaz, E. Yurtsever, I. Yilgör, Polymer 41 (2000) 849.
[34] a) C.M. Casado, M. Morán, J. Losada, I. Cuadrado, Inorg. Chem. 34 (1995) 1668;
b) C.M. Casado, I. Cuadrado, M. Morán, B. Alonso, F. Lobete, J. Losada, Organometallics 14 (1995) 2618;
c) M. Morán, C.M. Casado, I. Cuadrado, J. Losada, Organometallics 12 (1993) 4327.
[35] C.M. Casado, I. Cuadrado, M. Morán, B. Alonso, M. Barranco, J. Losada, Appl. Organometal. Chem. 13 (1999) 245.
[36] A.R. Petrov, K. Jess, M. Freytag, P.G. Jones, M. Tamm, Organometallics 32 (2013) 5946.
[37] CrysAlis RED, Oxford Diffraction Ltd., Version 1.171.34.76, 2003.
[38] O.V. Dolomanov, L.J. Bourhis, R.J. Gildea, J.A.K. Howard, H. Puschmann, J. Appl. Crystallogr. 42 (2009) 339.
[39] SHELXS G.M. Sheldrick, Acta Crystallogr., Part A 64 (2008) 112.
[40] W. Noll, Chemistry and Technology of Silicones, Academic Press, New York, London, 1968. p. 437–472.
[41] I. Yilgor, J.E. McGrath, Polysiloxane containing copolymers: a survey of recent developments, in: R. Stumpe (Ed.), Advances in Polymer Science, Polysiloxane Copolymers/Anionic Polymerization, vol. 86, Springer-Verlag, Berlin, 1988, pp. 1–86.
[42] L.R. Schroeder, S.L. Cooper, J. Appl. Phys. 47 (1976) 4310.
[43] D. Garcia, H.W. Starkweather, J. Polym. Sci: Polym. Phys. Ed. 23 (1985) 537.
[44] D.J. Skrovanek, S.E. Howe, P.C. Painter, M.M. Coleman, Macromolecules 18 (1985) 1676.
[45] D.J. Skrovanek, P.C. Painter, M.M. Coleman, Macromolecules 19 (1986) 699.
[46] M.M. Coleman, K.L. Lee, D.J. Skrovanek, P.C. Painter, Macromolecules 19 (1986) 2149.
[47] M.M. Coleman, D.J. Skrovanek, J. Hu, P.C. Painter, Macromolecules 21 (1988) 59.
[48] M.M. Coleman, M. Sobkowiak, G.J. Pehlert, P.C. Painter, Macromol. Chem. Phys. 198 (1997) 117.
[49] Y.L. Lu, G.B. Zhang, M. Feng, Y. Zhang, M.S. Yang, D.Y. Shen, J. Polym. Sci. B, Polym. Phys. 41 (2003) 2313.
[50] V.K. Sharma, S. Srivastava, Turk. J. Chem. 30 (2006) 755.